ELSEVIER

International Journal of Mass Spectrometry 222 (2003) 189–200

International Journal of Mass Spectrometry

www.elsevier.com/locate/ijms

Electron-impact total ionization cross-sections of the chlorofluoromethanes

Karl K. Irikura[a,*], M. Asgar Ali[b], Yong-Ki Kim[a]

[a] *National Institute of Standards and Technology, 100 Bureau Drive, Gaithersburg, MD 20899, USA*
[b] *Department of Chemistry, Howard University, Washington, DC 20059, USA*

Received 23 April 2002; accepted 11 September 2002

Abstract

Electron-impact total ionization cross-sections for CCl_3F (Freon 11), CCl_2F_2 (Freon 12), $CClF_3$ (Freon 13), $CHCl_2F$ (Freon 21), $CHClF_2$ (Freon 22), and CH_2ClF (Freon 31) are calculated using the Binary-Encounter-Bethe (BEB) theoretical model. The BEB model requires only binding energies and kinetic energies of molecular orbitals, as computed using standard molecular orbital program packages. Experimental cross-sections, where available, agree with the BEB results. All-electron ab initio calculations yield slightly larger BEB cross-sections than do pseudopotential calculations. (Int J Mass Spectrom 222 (2003) 189–200)
Published by Elsevier Science B.V.

Keywords: Ab initio; Chlorofluorocarbon; Effective core potential; Electron impact; Ionization cross-section; Plasma

1. Introduction

The chlorofluoromethanes CCl_3F and CCl_2F_2 are useful in a variety of applications. For example, dichlorodifluoromethane (Freon 12) is a refrigerant, a foam-blowing agent, an aerosol propellant, a plasma-processing gas and an additive in gaseous dielectric mixtures. However, these gases are also important in stratospheric ozone depletion [1]. Similar compounds that contain hydrogen atoms ($CH_nCl_xF_y$, $n > 0$) are finding use as temporary replacements, since they are more quickly scrubbed from the atmosphere by reactions with hydroxyl radicals [2].

Electron-impact ionization cross-sections are among the data necessary for modeling the plasma chemistry relevant to some applications.

For CCl_2F_2, Christophorou et al. have critically evaluated all physical quantities involving electron interactions [3]. Experimental measurements of the total ionization cross-section have been made by Beran and Kevan [4], Pejčev et al. [5], Leiter et al. [6], and Bart et al. [7]. For the other chlorofluoromethanes, the only published cross-sections are those by Beran and Kevan, reported for $CClF_3$, CCl_3F, $CHClF_2$, and $CHCl_2F$ at incident electron energies of 20, 35, and 70 eV [4], and those by Bart et al. for $CClF_3$ from threshold to 220 eV [7]. No data are available for CH_2ClF. In the present paper, we report total ionization cross-sections for all six chlorofluoromethanes at incident energies from threshold to 5000 eV. Cross-sections for fluoromethanes, $CH_{4-x}F_x$, and chloromethanes, $CH_{4-x}Cl_x$, are already available in the literature [7,8].

As will be elaborated in Section 5, different experimental research groups often disagree seriously on the

* Corresponding author. E-mail: karl.irikura@nist.gov

1387-3806/02/$ – see front matter. Published by Elsevier Science B.V.
PII S1387-3806(02)00981-8

values of total ionization cross-sections for molecules. Thus, a theory that is reliable to ±15% is quite attractive, especially for polyatomic or reactive molecules.

2. Theoretical background

Most schemes for predicting total electron-impact ionization cross-sections as a function of incident electron energy, $\sigma_i(T)$, involve many empirical parameters. The most successful such semi-empirical procedure is the "DM formalism" [9]. In contrast, the Binary-Encounter-Bethe (BEB) model was originally formulated without any empirical parameters [10]. For a wide range of molecules (e.g., H_2, SF_6, CF_4, C_2F_6, C_3F_8), non-empirical BEB theory produces σ_i values in good agreement (15% or better at the peak) with available experiments [11–17]. However, it was necessary to introduce one empirical parameter to obtain satisfactory results for molecules that contain atomic-like orbitals with principal quantum number $n \geq 3$ [11,18]. Likewise, a similar but non-parametric adjustment was found necessary for monopositive ions [10,18].

The BEB cross-section as a function of the kinetic energy of the incident electron, T, is computed as a sum over all molecular orbitals, $\sigma_i(T) = \sum_{MO}\sigma_{MO}(T)$, where

$$\sigma_{MO}(T) = \frac{S}{t + (u+1)/n} \times \left[\frac{\ln t}{2}\left(1 - \frac{1}{t^2}\right) + 1 - \frac{1}{t} - \frac{\ln t}{t+1}\right]. \quad (1)$$

In Eq. (1), $t = T/B$, $u = U/B$, $S = 4\pi a_0^2 N(R/B)^2$, a_0 is the Bohr radius, R the Rydberg energy, B, U, and N are the binding energy (i.e., the vertical ionization energy), the kinetic energy, and the occupation number, respectively, for the molecular orbital. If $T < B$, the incident electron does not have enough energy to ionize the orbital, so $\sigma_{MO} = 0$. In most cases, the constant n in Eq. (1) is unity. However, if the molecular orbital is dominated by atomic orbitals with principal quantum number ≥3 (as judged by a Mulliken population >50%), then n is set equal to the principal quantum number of the atomic orbital. This is an empirical adjustment, reflecting the observation that valence atomic orbitals with high principal quantum numbers have unusually high radial kinetic energies. The choice of threshold, taken here as 50%, is rather arbitrary. Table 1 shows the effect of choosing alternative thresholds of 75 and 25% instead. In the most extreme case (CCl_3F), reducing the threshold from 50 to 25% raises the peak cross-section by 10%. An alternative [19], which does not require any thresholds or adjustable parameters, is to use effective core potentials for high-Z atoms. This reduces the kinetic energy of the valence orbitals by eliminating the innermost radial nodes. For comparison, both approaches are employed in the present study.

Table 1
Peak ionization cross-sections (Å^2) computed using different Mulliken population thresholds (see Eq. (1))

	75%	50%	25%
CCl_3F	13.00	13.17	14.45
CCl_2F_2	10.43	11.01	11.34
$CClF_3$	8.13	8.13	8.46
$CHCl_2F$	10.15	10.74	11.33
$CHClF_2$	7.67	7.67	8.07
CH_2ClF	7.23	7.23	7.66

Removing an electron from a tightly bound orbital can lead to multiple ionization through an Auger mechanism. We assume that ionization of an orbital whose binding energy exceeds the second ionization energy of the molecule, $B > IE_2$, will always lead to double ionization. Since few doubly-charged molecules are stable, a double ionization event will generally produce two singly-charged fragment ions. Many experiments measure the total positive charge produced, rather than the number of ionization events. For comparison with such experiments, the contribution from orbitals with $B > IE_2$ is doubled. An approximate value of IE_2 is obtained from correlated ab initio calculations unless it is available from experiment. Triple and higher ionizations contribute little to the total ionization cross-section and are neglected here.

BEB theory assumes that all energy transfer in excess of the ionization threshold results in ionization.

However, molecules may dissociate into neutral fragments without ionization. Thus, BEB predictions are expected to overestimate σ_i by an amount corresponding to part of the total neutral dissociation caused by energy transfer exceeding the ionization threshold. Errors also result from the approximations in the ab initio calculations used to obtain the molecular orbital parameters B and U. For example, Hartree–Fock values of B are generally too high, leading to a reduction in the predicted cross-sections. BEB theory does not account for structured features such as autoionization.

In the present paper, we report BEB predictions for all six chlorofluoromethanes: CCl_3F, CCl_2F_2, $CClF_3$, $CHCl_2F$, $CHClF_2$, and CH_2ClF.

3. Details of molecular calculations

Molecular geometries were computed using the B3LYP hybrid density functional [20,21] in conjunction with the 6-31G(d) basis sets as implemented in the Gaussian 98 program suite [22,23]. All calculations on open-shell species were spin-unrestricted.

Orbital kinetic energies, U, were obtained from either all-electron or pseudopotential Hartree–Fock (HF) calculations. The all-electron calculations used the 6-311G(d,p) basis sets as implemented in the PC-GAMESS program [23–25]. The pseudopotential calculations, which were done using the MOLPRO program package [23,26], also used the 6-311G(d,p) basis sets for C, F, and H atoms, but used the ECP10MWB quasi-relativistic effective core potential (qRECP) on Cl atoms [27], which replaces the K and L shells. The valence basis set on Cl atoms was the corresponding ECP10MWB basis [27] contracted as (s31, p311) and supplemented by a set of d polarization functions with an exponent of $0.7a_0^{-2}$. Kinetic energies from pseudopotential calculations are relevant only for the valence orbitals.

Orbital binding energies, B, were obtained from the all-electron HF calculations, described above, for the core and inner valence orbitals. For the highest-lying (viz., the most weakly bound) orbital of each molecule, B was taken either from experimental measurements or from all-electron, frozen-core coupled-cluster CCSD(T) calculations [28,29] using cc-pVTZ basis sets [30,31] and executed using the ACES II [32] or Gaussian 98 program suite [23]. For the remaining valence orbitals, B was taken either from experiment or from outer-valence Green's function calculations (OVGF) [33,34] with 6-311+G(d,p) basis sets, as implemented in Gaussian 98.

Second ionization energies, IE_2, were taken as vertical energies for computational convenience, although the Auger step can be significantly slower than nuclear motion [35–38]. IE_2 values were computed by adding IE_v, obtained as described in the preceding paragraph, to the vertical ionization energy of the molecular cation at the geometry of the neutral molecule. This second quantity was computed using OVGF theory as described in the previous paragraph.

4. Results

The molecular orbital information for CCl_3F is collected in Table 2. Averaged experimental values [39–42] were adopted for the binding energies of the four highest-lying orbitals ($2a_2$, 10e, 9e, and $11a_1$), and are slightly higher than the CCSD(T) ($2a_2$ = 11.69 eV) and OVGF (11.56, 11.96, 12.72, and 13.10 eV, respectively) binding energies. The HF values are much higher: 12.75, 13.13, 13.96, and 14.36 eV, respectively. OVGF binding energies were adopted for the next four orbitals (pole strengths $\geq$ 0.87). Double ionization was assumed for orbitals $8a_1$ and below (i.e., larger B), based upon the experimental vertical double ionization energy of 30.9 ± 0.5 eV [43]. Orbital 6e was excluded from double ionization because its binding energy is expected to drop by 2–3 eV in a correlated calculation. The four highest orbitals correspond to the six chlorine 3pπ lone pairs (at least 92% Cl 3p character based upon Mulliken analysis) and were treated with $n = 3$ in Eq. (1). Orbitals 6e and $8a_1$ have 90 and 67% Cl 3s character, respectively, and were also treated with $n = 3$. Kinetic energies obtained using the pseudopotential method are listed parenthetically in Table 2 and are

Table 2
Molecular orbital binding and kinetic energies for CCl_3F and CCl_2F_2

CCl_3F (C_{3v})			CCl_2F_2 (C_{2v})		
Orbital	B (eV)	U (eV)	Orbital	B (eV)	U (eV)
$2a_2$	11.8	68.22[a] (26.75)	$8b_1$	12.24	66.86[a] (26.42)
10e	12.2	65.86[a] (26.43)	$3a_2$	12.54	66.03[a] (27.45)
9e	13.0	63.56[a] (27.45)	$6b_2$	13.08	64.02[a] (28.15)
$11a_1$	13.5	61.53[a] (27.17)	$12a_1$	13.50	61.48[a] (26.02)
8e	15.00	66.80 (42.37)	$7b_1$	14.36	74.22[a] (56.84)
7e	18.46	75.56 (67.43)	$11a_1$	16.29	73.68 (62.90)
$10a_1$	18.46	66.19 (44.91)	$5b_2$	16.41	92.65 (92.15)
$9a_1$	22.21	80.24 (60.05)	$2a_2$	17.21	86.93 (86.55)
6e	30.91	79.06[a] (15.61)	$6b_1$	19.44	74.07 (48.69)
$8a_1$	33.76	66.93[a] (24.51)	$10a_1$	19.51	74.04 (63.95)
$7a_1$	46.34	98.58	$4b_2$	20.62	77.62 (76.36)
4e	219.7	561.92	$9a_1$	23.35	83.25 (69.02)
$6a_1$	219.7	561.93	$5b_1$	31.07	77.79[a] (16.03)
$1a_2$	219.7	561.93	$8a_1$	32.91	72.08[a] (25.53)
5e	219.7	561.93	$3b_2$	45.51	105.25
3e	219.79	560.78	$7a_1$	47.42	93.53
$5a_1$	219.79	560.77	$1a_2$	219.75	562.02
$4a_1$	288.68	593.37	$2b_2$	219.75	562.02
2e	288.69	593.35	$4b_1$	219.75	562.02
$3a_1$	313.98	436.69	$6a_1$	219.75	562.03
$2a_1$	717.61	1013.44	$3b_1$	219.84	560.90
1e	2854.01	3731.11	$5a_1$	219.84	560.90
$1a_1$	2854.01	3731.11	$2b_1$	288.73	593.30
			$4a_1$	288.73	593.32
			$3a_1$	314.78	436.58
			$1b_2$	717.75	1013.42
			$2a_1$	717.75	1013.43
			$1b_1$	2854.05	3731.11
			$1a_1$	2854.05	3731.11

Kinetic energies from pseudopotential calculations are listed parenthetically.
[a] $n = 3$ in Eq. (1).

always treated with $n = 1$. Occupation numbers are $N = 2$ for orbitals of a_1 and a_2 symmetry and $N = 4$ for orbitals of e symmetry (C_{3v} point group). The BEB cross-sections are plotted in Fig. 1; the solid curve is from all-electron kinetic energies and the dashed curve is from pseudopotential-derived kinetic energies.

The molecular orbital data for CCl_2F_2 are listed in Table 2. Experimental values for the binding energies of the five highest-lying orbitals ($8b_1$, $3a_2$, $6b_2$, $12a_1$, and $7b_1$) were taken from the most recent [44] of four experimental measurements [39–41,44]. These values are slightly higher than the CCSD(T) ($8b_1 = 12.09$ eV, $3a_2 = 12.46$ eV) and OVGF (11.96, 12.33, 12.84, 13.15, and 14.18 eV, respectively) binding energies. The HF values are much higher: 13.07, 13.51, 14.03, 14.34, and 15.50 eV, respectively. OVGF binding energies were adopted for the next seven orbitals (pole strengths ≥ 0.88). Double ionization was assumed for orbitals $8a_1$ and below, based upon the experimental vertical double ionization energy of 31.6 ± 0.5 eV [43]. The four highest orbitals correspond to the four chlorine $3p\pi$ lone pairs (at least 93% Cl 3p character) and were treated with $n = 3$ in Eq. (1). Orbitals $5b_1$ and $8a_1$ have 88 and 70% Cl 3s character, respectively, and were also treated with $n = 3$. Orbital $7b_1$ has 57% Cl valence character and was treated with $n = 3$. Kinetic energies obtained using the pseudopotential method are listed parenthetically in Table 2 and are always treated with $n = 1$. Occupation numbers

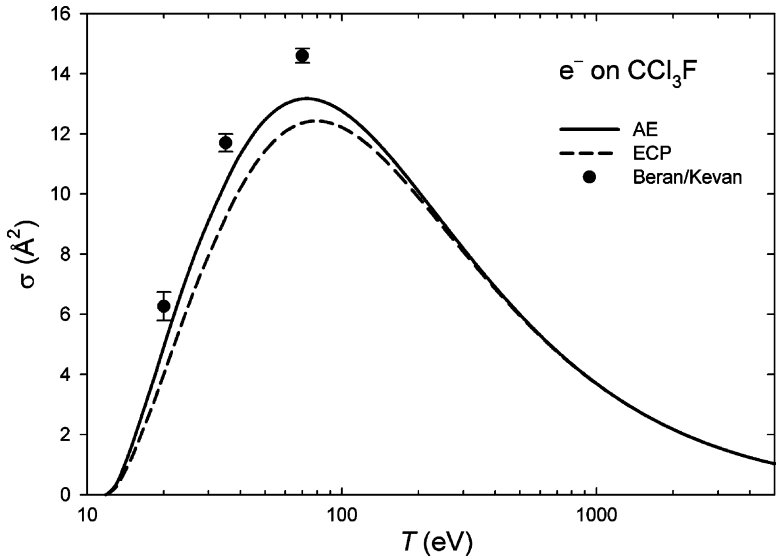

Fig. 1. Total electron-impact ionization cross-section for CCl_3F. Points are from experiment and curves are from all-electron (AE) or effective core potential (ECP) BEB theory. The experimental error-bars only include statistical uncertainties.

are $N = 2$ for all orbitals (C_{2v} point group). The BEB cross-sections are plotted in Fig. 2; the solid curve is from all-electron kinetic energies and the dashed curve is from pseudopotential-derived kinetic energies.

The molecular orbital data for $CClF_3$ are listed in Table 3. Averaged experimental values [39–41] were used for the binding energies of the five highest-lying orbitals (7e, $10a_1$, $1a_2$, 6e, and 5e), and differ erratically from the corresponding CCSD(T) (7e = 12.85 eV) and OVGF (12.77, 14.99, 16.21, 16.87, and 17.92 eV, respectively) binding energies. The HF values are much higher: 13.85, 16.29, 18.65, 19.12, and 20.33 eV, respectively. OVGF binding energies were adopted for the next three orbitals (pole strengths $\geq$ 0.89). Double ionization was assumed for orbitals 3e and below, based upon the experimental vertical double ionization energy of 35.4 ± 0.5 eV [43]. The highest (viz., most weakly bound) orbital, 7e, corresponds to the two chlorine 3pπ lone pairs (95% Cl 3p character) and was treated with $n = 3$ in Eq. (1). Orbital $7a_1$ has 76% Cl 3s character and was also treated with $n = 3$. Orbital $10a_1$ has only 49% Cl 3p character and was treated with $n = 1$. Kinetic energies obtained using the pseudopotential method are listed parenthetically in Table 3 and are always treated with $n = 1$. Occupation numbers are $N = 2$ for orbitals of a_1 and a_2 symmetry and $N = 4$ for orbitals of e symmetry (C_{3v} point group). The BEB cross-sections are plotted in Fig. 3; the solid curve is from all-electron kinetic energies and the dashed curve is from pseudopotential-derived kinetic energies.

Molecular orbital data for $CHCl_2F$ are included in Table 3. Experimental values [45] were used for the binding energies of the four highest-lying orbitals (10a″, 15a′, 9a″, and 14a′), and are somewhat higher than the corresponding CCSD(T) (10a″ = 11.77 eV) and OVGF (11.65, 12.02, 12.11, and 12.69 eV, respectively) binding energies. Note that the experimental values for the first two orbitals (10a″ and 15a′) are from unresolved peaks, so may be skewed to higher binding energy. The HF values are much higher: 12.67, 13.06, 13.20, and 13.79 eV, respectively. OVGF binding energies were adopted for the next six orbitals (8a″, 13a′, 12a′, 7a″, 11a′, and 10a′; pole strengths $\geq$ 0.87). Double ionization was assumed for orbitals 9a′ and below, based upon the vertical double ionization energy of 29.8 eV, computed as described in Section 3. Orbital 6a″ was excluded from double ionization

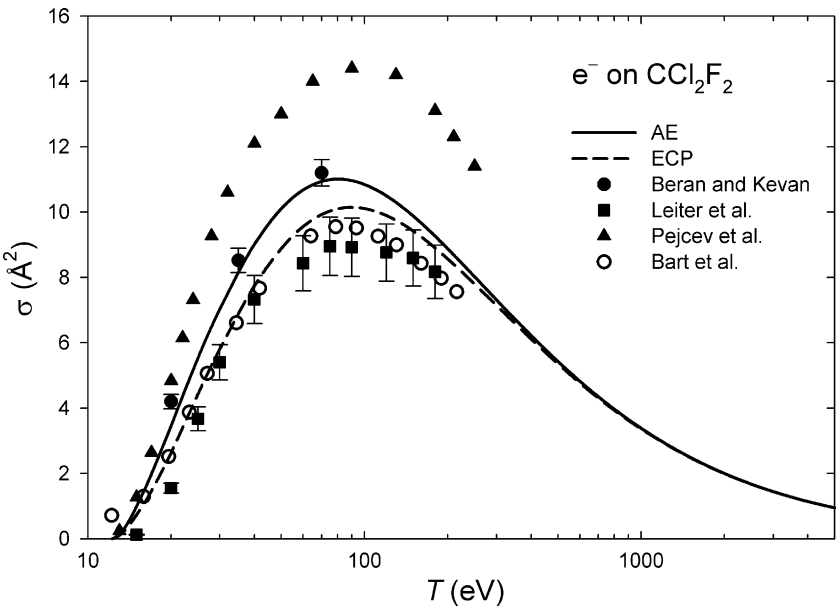

Fig. 2. Total electron-impact ionization cross-section for CCl_2F_2. Points are from experiment and curves are from all-electron (AE) or effective core potential (ECP) BEB theory. The experimental error-bars reflect only statistical uncertainties in the case of [4] and were estimated total uncertainties of ±10% in [6].

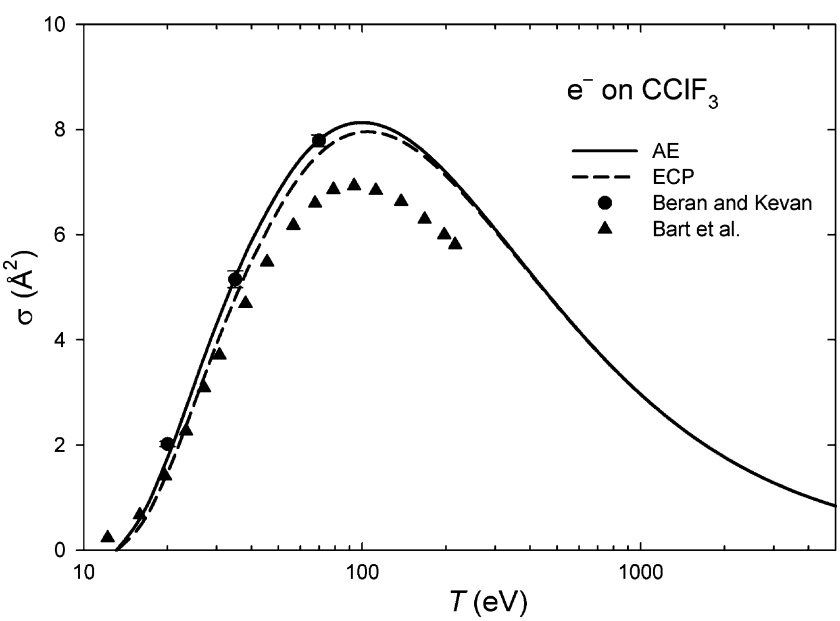

Fig. 3. Total electron-impact ionization cross-section for $CClF_3$. Points are from experiment and curves are from all-electron (AE) or effective core potential (ECP) BEB theory. The experimental error-bars only include statistical uncertainties.

Table 3
Molecular orbital binding and kinetic energies for $CClF_3$ and $CHCl_2F$

$CClF_3$ (C_{3v})			$CHCl_2F$ (C_s)		
Orbital	B (eV)	U (eV)	Orbital	B (eV)	U (eV)
7e	13.10	64.62[a] (27.79)	10a″	11.92	66.07[a] (26.20)
$10a_1$	15.12	75.61 (54.40)	15a′	12.12	60.31[a] (26.87)
$1a_2$	15.7	95.03 (95.07)	9a″	12.37	64.22[a] (26.38)
6e	16.68	91.05 (90.87)	14a′	12.97	62.05[a] (27.16)
5e	17.6	85.33 (85.08)	8a″	14.39	67.97[a] (42.40)
$9a_1$	20.30	72.97 (61.15)	13a′	14.95	63.90 (48.99)
4e	21.46	75.96 (75.62)	12a′	17.90	72.25 (60.15)
$8a_1$	24.38	84.17 (76.32)	7a″	17.96	76.43 (69.49)
$7a_1$	32.17	75.06[a] (23.63)	11a′	19.22	61.02 (59.64)
3e	45.68	104.85	10a′	22.70	68.93 (49.35)
$6a_1$	48.36	90.81	6a″	30.46	79.50[a] (15.41)
2e	219.82	561.70	9a′	32.63	67.90[a] (23.33)
$5a_1$	219.91	560.59	8a′	45.62	99.15
$4a_1$	288.80	593.33	4a″	219.29	561.87
$3a_1$	315.57	436.69	6a′	219.29	561.87
$2a_1$	717.84	1013.44	5a″	219.29	561.88
$1a_1$	2854.12	3731.10	7a′	219.29	561.88
			3a″	219.38	560.82
			5a′	219.38	560.81
			2a″	288.27	593.33
			4a′	288.27	593.34
			3a′	312.18	436.49
			2a′	717.06	1013.44
			1a″	2853.59	3731.11
			1a′	2853.59	3731.11

Kinetic energies from pseudopotential calculations are listed parenthetically.
[a] $n = 3$ in Eq. (1).

because its binding energy is expected to drop by 2–3 eV in a correlated calculation. The highest four orbitals correspond to the four chlorine 3pπ lone pairs (99, 87, 98, and 93% Cl 3p character, respectively) and were treated with $n = 3$ in Eq. (1). Orbitals 9a′ and 6a″ have 91% and 69% Cl 3s character, respectively, and were also treated with $n = 3$. Orbital 8a″ has 60% Cl valence character and was treated with $n = 3$. Kinetic energies obtained using the pseudopotential method are listed parenthetically in Table 3 and are always treated with $n = 1$. Occupation numbers are $N = 2$ for all orbitals (C_s point group). The BEB cross-sections are plotted in Fig. 4; the solid curve is from all-electron kinetic energies and the dashed curve is from pseudopotential-derived kinetic energies.

Molecular orbital data for $CHClF_2$ are included in Table 4. The only experimentally resolved peaks, and therefore the only reliable binding energies, are at 13.91 and 18.87 eV for the third (13a′) and seventh (11a′) highest orbitals, respectively [45]. The corresponding OVGF values are 13.91 and 18.90 eV, in good agreement. Thus, we use the OVGF values for orbitals 3–10 (13a′ through 9a′; pole strengths ≥ 0.87). For the highest two orbitals (14a′ and 7a″), we adopt the CCSD(T) values of 12.35 and 12.40 eV, slightly higher than the corresponding OVGF values (12.25 and 12.31 eV). The HF values for the highest 10 orbitals are 13.21, 13.31, 15.07, 17.86, 18.24, 19.17, 21.10, 21.91, 22.49, and 26.20 eV, respectively. Double ionization was assumed for orbitals 3a″ and below, based upon the vertical double ionization energy of 33.5 eV, computed as described in Section 3. The two highest orbitals, 14a′ and 7a″, correspond to the chlorine 3pπ lone pairs (94 and 95% Cl 3p character,

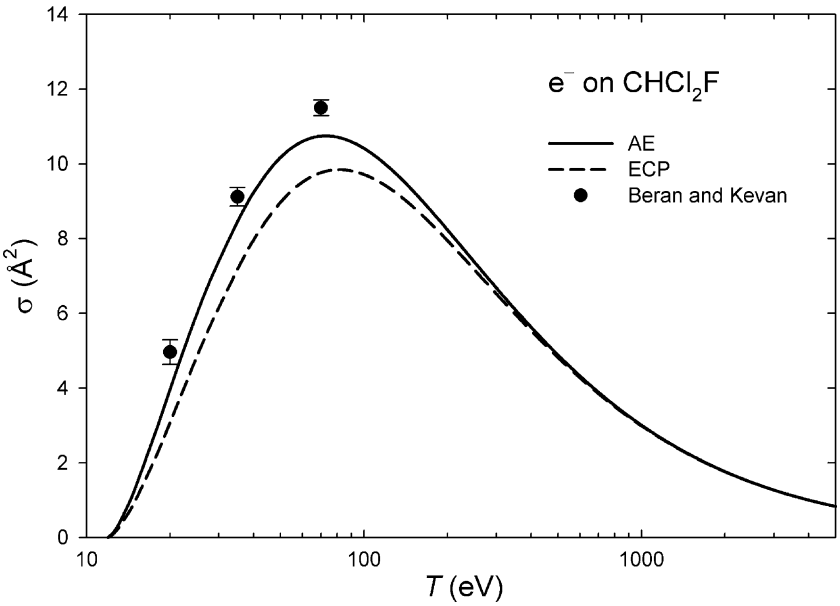

Fig. 4. Total electron-impact ionization cross-section for $CHCl_2F$. Points are from experiment and curves are from all-electron (AE) or effective core potential (ECP) BEB theory. The experimental error-bars only include statistical uncertainties.

Table 4
Molecular orbital binding and kinetic energies for $CHClF_2$ and CH_2ClF

$CHClF_2$ (C_s)			CH_2ClF (C_s)		
Orbital	*B* (eV)	*U* (eV)	Orbital	*B* (eV)	*U* (eV)
14a′	12.35	61.63[a] (25.89)	4a″	11.66	60.16[a] (26.62)
7a″	12.40	63.97[a] (27.53)	13a′	12.03	62.15[a] (26.06)
13a′	13.91	69.02 (50.35)	12a′	13.78	64.07 (43.12)
6a″	16.03	92.07 (91.99)	3a″	14.59	60.95 (57.79)
12a′	16.08	74.33 (69.74)	11a′	17.25	75.17 (68.07)
5a″	16.78	87.64 (87.40)	10a′	18.30	65.42 (64.55)
11a′	18.90	74.24 (65.66)	2a″	18.42	56.29 (55.67)
4a″	20.01	77.65 (77.21)	9a′	23.16	61.69 (45.51)
10a′	20.33	60.07 (59.72)	8a′	31.06	70.17[a] (21.17)
9a′	23.81	72.65 (60.79)	7a′	44.64	99.71
8a′	31.56	73.48[a] (22.90)	6a′	218.67	561.76
3a″	44.79	105.27	1a″	218.67	561.80
7a′	46.58	94.75	5a′	218.75	560.81
2a″	219.21	561.68	4a′	287.65	593.31
6a′	219.21	561.69	3a′	310.16	436.30
5a′	219.30	560.68	2a′	716.28	1013.43
4a′	288.19	593.31	1a′	2852.97	3731.10
3a′	312.90	436.50			
1a″	717.11	1013.43			
2a′	717.11	1013.44			
1a′	2853.51	3731.10			

Kinetic energies from pseudopotential calculations are listed parenthetically.
[a] $n = 3$ in Eq. (1).

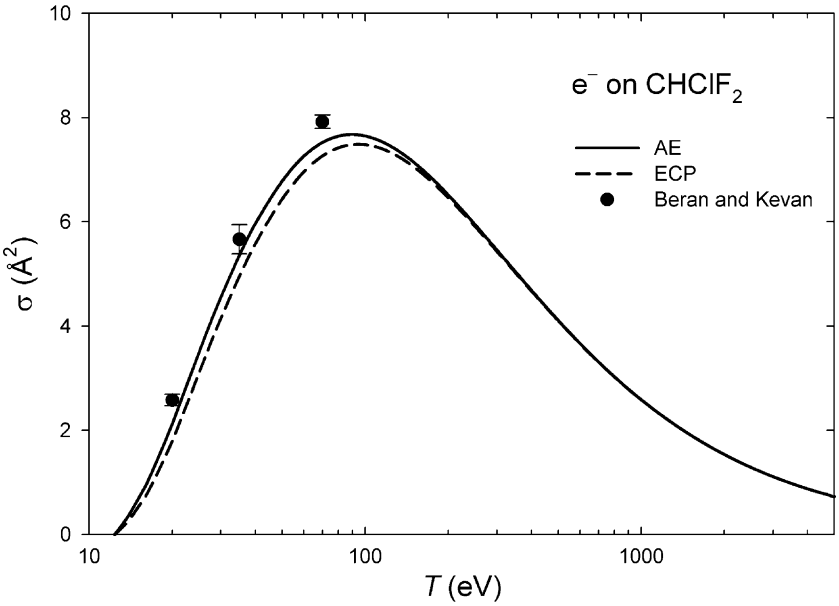

Fig. 5. Total electron-impact ionization cross-section for $CHClF_2$. Points are from experiment and curves are from all-electron (AE) or effective core potential (ECP) BEB theory. The experimental error-bars only include statistical uncertainties.

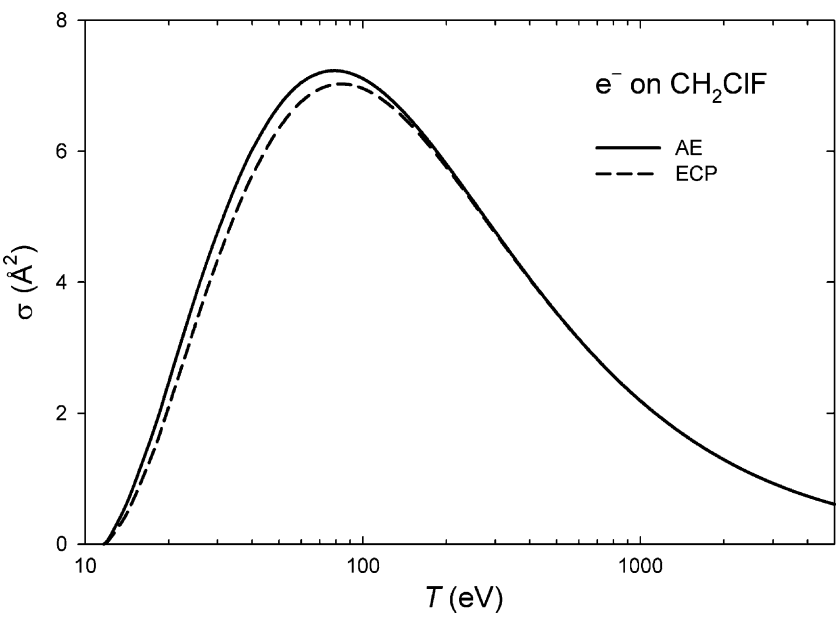

Fig. 6. Total electron-impact ionization cross-section for CH_2ClF from all-electron (AE) or effective core potential (ECP) BEB theory.

respectively) and were treated with $n = 3$ in Eq. (1). Orbital 8a′ has 75% Cl 3s character and was also treated with $n = 3$. Kinetic energies obtained using the pseudopotential method are listed parenthetically in Table 4 and are always treated with $n = 1$. Occupation numbers are $N = 2$ for all orbitals (C_s point group). The BEB cross-sections are plotted in Fig. 5; the solid curve is from all-electron kinetic energies and the dashed curve is from pseudopotential-derived kinetic energies.

Molecular orbital data for CH_2ClF are included in Table 4. No experimental binding energies are available. We accept the CCSD(T) binding energies for the two highest orbitals (4a″ and 13a′) and OVGF values for the next six orbitals (12a′ through 9a′; pole strengths ≥ 0.87). For comparison, the OVGF binding energies for the two highest orbitals are 11.54 and 11.90 eV. The HF values for the highest eight orbitals are 12.42, 12.80, 14.72, 16.08, 19.13, 20.08, 20.49, and 25.53 eV, respectively. Double ionization was assumed for orbitals 7a′ and below, based upon the vertical double ionization energy of 32.2 eV, computed as described in Section 3. The two highest orbitals, 4a″ and 13a′, correspond to the chlorine 3pπ lone pairs (87 and 95% Cl 3p character, respectively) and were treated with $n = 3$ in Eq. (1). Orbital 8a′ has 73% Cl 3s character and was also treated with $n = 3$. Kinetic energies obtained using the pseudopotential method are listed parenthetically in Table 4 and are always treated with $n = 1$. Occupation numbers are $N = 2$ for all orbitals (C_s point group). The BEB cross-sections are plotted in Fig. 6; the solid curve is from all-electron kinetic energies and the dashed curve is from pseudopotential-derived kinetic energies.

5. Discussion

5.1. Comparison between all-electron and effective core potential calculations

As described in Section 2, there are two procedures for adjusting kinetic energies when high-*n* (i.e., $n \geq 3$) atomic orbitals are involved. In the "all-electron" (AE) procedure, if a molecular orbital is predominately composed of high-*n* atomic orbitals, the corresponding value of *n* is used in Eq. (1). Otherwise, $n = 1$ is used. In the "effective core potential" (ECP) procedure, the core electrons of each high-*Z* atom are replaced by an effective potential. The ECP removes the orthogonality constraints that cause the inner radial nodes in the valence orbitals, thus reducing their kinetic energies. For all six molecules in this study, the ECP cross-section is significantly (15–24%) smaller than the AE value at 20 eV, i.e., near the threshold. This difference narrows with increasing incident energy. At the peak in the cross-section, the ECP value is only 2–8% lower than the AE result. As expected, the difference is generally larger for molecules with greater numbers of high-*n* orbitals. The two procedures agree closely for incident electron energies of a few hundred eV and higher. Unfortunately, the available experimental data are too discordant (Fig. 2) to allow us to judge whether the AE model or the ECP model is superior.

5.2. Comparison between theory and experiment and among experiments

Beran and Kevan reported experimental cross-sections (at $T = 20$, 35, and 70 eV) for five of the six molecules in the present study [4]. Compared with their results, the BEB cross-sections at 20 eV are too low by 13–22% (AE) or by 27–38% (ECP). Agreement improves at higher incident energy; at 70 eV the BEB predictions appear too low by 10% or less (AE) or by 15% or less (ECP). For the CCl_2F_2 molecule, cross-sections have also been measured by Pejčev et al. [5], by Leiter et al. [6], and by Bart et al. [7]. At 20 eV, these later measurements differ from the earliest by +15, −63, and −37%, respectively. At 70 eV, the differences are +27, −22, and −16%. This is illustrated in Fig. 2. Likewise, for $CClF_3$, the measurements by Bart et al. differ from those by Beran and Kevan by −26% at 20 eV and −14% at 70 eV (Fig. 3).

These examples illustrate the difficulty of obtaining consistent experimental results. Measurements on noble gases are expected to be more reliable than

for molecules because these gases are easily purified, chemically inert, easily managed in ultra-high vacuum equipment, and suffer no fragmentation upon ionization. For example, argon often serves as a benchmark system for measurements of electron-impact ionization cross-sections of molecules. Nonetheless, the scatter among the most reliable published cross-sections for Ar, as identified by Rejoub et al. [46], is about ±3.5% at peak, ±5% at 50 eV, and ±9% at 20 eV [46–49]. The situation for molecular cross-sections is worse. For example, the experimental disagreement for CCl_2F_2 (Fig. 2) amounts to ±23% about the mean at the peak and ±50% about the mean at 20 eV. Thus, we conclude that the BEB predictions are no worse than typical experimental measurements on molecules. Agreement between BEB theory and experiment, and also among different experimental groups, is worst at the lowest incident electron energies.

6. Conclusions

We have presented total cross-sections for electron-impact ionization of the six chlorofluoromethanes, as computed using BEB theory. BEB parameters were obtained from ab initio calculations, either using an effective core potential (ECP) or with all electrons explicit (AE). The ECP calculations yield somewhat smaller cross-sections than the AE calculations, but additional studies will be needed before either procedure can be declared superior. The reliability of the BEB predictions is about the same as that of typical experimental measurements.

Acknowledgements

We are grateful to Prof. Peter Harland for providing numerical cross-section data for CCl_2F_2 and $CClF_3$.

References

[1] S. Solomon, Rev. Geophys. 37 (1999) 275.
[2] A.R. Ravishankara, E.R. Lovejoy, J. Chem. Soc., Faraday Trans. 90 (1994) 2159.
[3] L.G. Christophorou, J.K. Olthoff, Y. Wang, J. Phys. Chem. Ref. Data 26 (1997) 1205.
[4] J.A. Beran, L. Kevan, J. Phys. Chem. 73 (1969) 3866.
[5] V.M. Pejčev, M.V. Kurepa, I.M. Cadez, Chem. Phys. Lett. 63 (1979) 301.
[6] K. Leiter, P. Scheier, G. Walder, T.D. Märk, Int. J. Mass Spectrom. Ion Process. 87 (1989) 209.
[7] M. Bart, P.W. Harland, J.E. Hudson, C. Vallance, Phys. Chem. Chem. Phys. 3 (2001) 800.
[8] I. Torres, R. Martínez, M.N. Sánchez Rayo, F. Castaño, J. Chem. Phys. 115 (2001) 4041.
[9] M. Probst, H. Deutsch, K. Becker, T.D. Märk, Int. J. Mass Spectrom. 206 (2001) 13.
[10] Y.-K. Kim, M.E. Rudd, Phys. Rev. A 50 (1994) 3954.
[11] W. Hwang, Y.-K. Kim, M.E. Rudd, J. Chem. Phys. 104 (1996) 2956.
[12] Y.-K. Kim, W. Hwang, N.M. Weinberger, M.A. Ali, M.E. Rudd, J. Chem. Phys. 106 (1997) 1026.
[13] M.A. Ali, Y.-K. Kim, W. Hwang, N.M. Weinberger, M.E. Rudd, J. Chem. Phys. 106 (1997) 9602.
[14] Y.-K. Kim, M.A. Ali, M.E. Rudd, J. Res. Natl. Inst. Stand. Technol. 102 (1997) 693.
[15] H. Nishimura, W.M. Huo, M.A. Ali, Y.-K. Kim, J. Chem. Phys. 110 (1999) 3811.
[16] M.A. Ali, K.K. Irikura, Y.-K. Kim, Int. J. Mass Spectrom. 201 (2000) 187.
[17] Y.-K. Kim, K.K. Irikura, M.A. Ali, J. Res. Natl. Inst. Stand. Technol. 105 (2000) 285.
[18] Y.-K. Kim, K.K. Irikura, Electron-impact ionization cross-sections for polyatomic molecules, radicals, and ions, in: K.A. Berrington, K.L. Bell (Eds.), Atomic and Molecular Data and Their Applications, vol. CP543, American Institute of Physics, College Park, MD, 2000, p. 220.
[19] W.M. Huo, Y.-K. Kim, Chem. Phys. Lett. 319 (2000) 576.
[20] A.D. Becke, J. Chem. Phys. 98 (1993) 5648.
[21] P.J. Stephens, F.J. Devlin, C.F. Chabalowski, M.J. Frisch, J. Phys. Chem. 98 (1994) 11623.
[22] M.J. Frisch, G.W. Trucks, H.B. Schlegel, G.E. Scuseria, M.A. Robb, J.R. Cheeseman, V.G. Zakrzewski, J.A. Montgomery Jr., R.E. Stratmann, J.C. Burant, S. Dapprich, J.M. Millam, A.D. Daniels, K.N. Kudin, M.C. Strain, O. Farkas, J. Tomasi, V. Barone, M. Cossi, R. Cammi, B. Mennucci, C. Pomelli, C. Adamo, S. Clifford, J. Ochterski, G.A. Petersson, P.Y. Ayala, Q. Cui, K. Morokuma, D.K. Malick, A.D. Rabuck, K. Raghavachari, J.B. Foresman, J. Cioslowski, J.V. Ortiz, B.B. Stefanov, G. Liu, A. Liashenko, P. Piskorz, I. Komaromi, R. Gomperts, R.L. Martin, D.J. Fox, T. Keith, M.A. Al-Laham, C.Y. Peng, A. Nanayakkara, C. Gonzalez, M. Challacombe, P.M.W. Gill, B. Johnson, W. Chen, M.W. Wong, J.L. Andres, C. Gonzalez, M. Head-Gordon, E.S. Replogle, J.A. Pople, Gaussian 98, Gaussian, Inc., Pittsburgh, PA, 1998.
[23] Certain commercial materials and equipment are identified in this paper in order to specify procedures completely. In no case does such identification imply recommendation or endorsement by the National Institute of Standards and Technology, nor does it imply that the material or equipment identified is necessarily the best available for the purpose.

[24] M.W. Schmidt, K.K. Baldridge, J.A. Boatz, S.T. Elbert, M.S. Gordon, J.H. Jensen, S. Koseki, N. Matsunaga, K.A. Nguyen, S.J. Su, T.L. Windus, M. Dupuis, J.A. Montgomery, J. Comput. Chem. 14 (1993) 1347.
[25] A.A. Granovsky, PC-GAMESS, 6.0, Moscow State University, Moscow, 2000.
[26] MOLPRO is a package of ab initio programs written by H.-J. Werner, P.J. Knowles, with contributions from R.D. Amos, A. Bernhardsson, A. Berning, P. Celani, D.L. Cooper, M.J.O. Deegan, A.J. Dobbyn, F. Eckert, C. Hampel, G. Hetzer, T. Korona, R. Lindh, A.W. Lloyd, S.J. McNicholas, F.R. Manby, W. Meyer, M.E. Mura, A. Nicklass, P. Palmieri, R. Pitzer, G. Rauhut, M. Schütz, H. Stoll, A.J. Stone, R. Tarroni, T. Thorsteinsson.
[27] A. Bergner, M. Dolg, W. Küchle, H. Stoll, H. Preuß, Mol. Phys. 80 (1993) 1431.
[28] G.D. Purvis, R.J. Bartlett, J. Chem. Phys. 76 (1982) 1910.
[29] K. Raghavachari, G.W. Trucks, J.A. Pople, M. Head-Gordon, Chem. Phys. Lett. 157 (1989) 479.
[30] T.H. Dunning Jr., J. Chem. Phys. 90 (1989) 1007.
[31] D.E. Woon, T.H. Dunning Jr., J. Chem. Phys. 98 (1993) 1358.
[32] J.F. Stanton, J. Gauss, J.D. Watts, M. Nooijen, N. Oliphant, S.A. Perera, P.G. Szalay, W.J. Lauderdale, S.A. Kucharski, S.R. Gwaltney, S. Beck, A. Balková, D.E. Bernholdt, K.-K. Baeck, P. Rozyczko, H. Sekino, C. Hober, R.J. Bartlett, ACES II, release 3.0, is a program product of the Quantum Theory Project, University of Florida, Integral packages included are VMOL (J. Almlöf and P.R. Taylor); VPROPS (P. Taylor); ABACUS (T. Helgaker, H.J. Aa. Jensen, P. Jørgensen, J. Olsen, and P.R. Taylor).
[33] W. von Niessen, J. Schirmer, L.S. Cederbaum, Comput. Phys. Rep. 1 (1984) 57.
[34] V.G. Zakrzewski, J.V. Ortiz, J. Phys. Chem. 100 (1996) 13979.
[35] J.H.D. Eland, P. Lablanquie, M. Lavollée, M. Simon, R.I. Hall, M. Hochlaf, F. Penent, J. Phys. B At. Mol. Opt. Phys. 30 (1997) 2177.
[36] B. Kempgens, A. Kivimäki, B.S. Itchkawitz, H.M. Köppe, M. Schmidbauer, M. Neeb, K. Maier, J. Feldhaus, A.M. Bradshaw, J. Electron Spectrosc. Relat. Phenom. 93 (1998) 39.
[37] S. Hsieh, J.H.D. Eland, J. Phys. B At. Mol. Opt. Phys. 29 (1996) 5795.
[38] S.D. Price, J.H.D. Eland, J. Phys. B At. Mol. Opt. Phys. 24 (1991) 4379.
[39] H.W. Jochims, W. Lohr, H. Baumgärtel, Ber. Bunsenges. Phys. Chem. 80 (1976) 130.
[40] R. Jadrny, L. Karlsson, L. Mattsson, K. Siegbahn, Phys. Scr. 16 (1977) 235.
[41] T. Cvitas, H. Güsten, L. Klasinc, J. Chem. Phys. 67 (1977) 2687.
[42] C. Cauletti, C. Puliti, J. Kreile, H.-D. Kurland, A. Schweig, V.I. Nefedov, J. Electron Spectrosc. Relat. Phenom. 46 (1988) 405.
[43] M.L. Langford, F.M. Harris, C.J. Reid, J.A. Ballantine, D.E. Parry, Int. J. Mass Spectrom. Ion Process. 112 (1992) 285.
[44] T. Pradeep, D.A. Shirley, J. Electron Spectrosc. Relat. Phenom. 66 (1993) 125.
[45] I. Novak, T. Cvitas, L. Klasinc, H. Güsten, J. Chem. Soc., Faraday Trans. II 77 (1981) 2049.
[46] R. Rejoub, B.G. Lindsay, R.F. Stebbings, Phys. Rev. A 65 (2002) 042713.
[47] D. Rapp, P. Englander-Golden, J. Chem. Phys. 43 (1965) 1464.
[48] J. Fletcher, I.R. Cowling, J. Phys. B 6 (1973) L258.
[49] R.C. Wetzel, F.A. Baiocchi, T.R. Hayes, R.S. Freund, Phys. Rev. A 35 (1987) 559.